Design Optimization of a Soft Gripper using Self-Contacts

Tanguy Navez, Baptiste Liévin, Quentin Peyron, Stefan Escaida Navarro, Olivier Goury, Christian Duriez

Design Optimization of a Soft Gripper using Self-Contacts

Tanguy Navez*, Baptiste Liévin*, Quentin Peyron*, Stefan Escaida Navarro *†,
Olivier Goury* and Christian Duriez*

***Abstract*— The design of soft robots' deformable bodies is complex, partly due to the trade-off between softness for motion and stiffness for force generation. Self-contacts in soft structures can be used to address this problem but have been marginally investigated. In parallel, parametric designs and computational optimization tools constitute an important trend paving the way toward shareable and reproducible results. In this paper, we study the potential of self-contacts in the design of soft grippers using a multi-objective design optimization environment. This open-source environment is targeted toward grasping tasks and is used both for design and model calibration. Soft fingers with improved grasping quality and energy are obtained, taking into account different friction coefficients at the contacts and different shapes of the objects to grasp. They are experimentally validated in terms of mechanical behavior and grasping performances.**

I. Introduction

Soft robots take advantage of compliant materials for flexible interactions with their environment. Their ability to reconfigure their shape and conform to hard objects makes them ideal candidates for manipulation tasks. Designing and assessing both soft grippers and soft manipulators is a broad area of research getting more and more attention from the soft robotics community [1] [2].

A soft gripper design is classically optimized in a multi-objective setting. However, the design task is difficult regarding the stiffness of the deformable part. The latter has to be able to easily reach the object to be handled while transmitting significant forces for grasping and handling. On the one hand, a consistently flexible manipulator will easily reach the object but will eventually fail to pick it up. On the other hand, a constantly stiffer manipulator will require a lot of effort and energy just to reach the object. Similarly, developing soft grippers capable of generating a desired grasping force requires them to be soft enough to conform to the object shape and maximize the contact area, and rigid enough to transfer loads. Therefore a compromise has to be found between the abilities of the gripper both to deform during the grasping phase and to stiffen during object manipulation.

Satisfying these requirements has been addressed through active stiffness modulation [3]. Another interesting approach is to leverage self-contacts. These can be used to create closed parallel chains for specific actuation values and therefore stiffen the structure. Few works consider using self-contacts in their soft robot design. One famous example is the design of a fast PneuNet actuator developed in [4]. The actuator is composed of an inextensible layer deformed by a series of cube-like chambers, whose walls collide upon inflation to create additional forces. In [5], a bio-inspired soft manipulator robot based on a compliant spine uses self-collision of its vertebrae to limit local deformations. Finally, a catheter made with several segments with joint stops is introduced in [6] that can stiffen locally and achieve a desired shape for the same actuation force. These soft robot designs exploit a-posteriori self-collisions and there is no general methodology to design soft robots using self-contacts. Moreover, there is, to the best of our knowledge, no analysis of the influence of self-contacts on the robot behavior and their potential for designing grippers and manipulators.

Given the trend toward computational design in soft robotics, there is a growing interest for sharing parametric families of designs coupled with simulation tools, that can be easily adapted to the user needs through computational optimization. Few works on design optimization frameworks targeting contact-aided soft robot design have been proposed. In [7], design optimization of contact-aided continuum robots is addressed. In the field of compliant mechanisms synthesis, a computational framework has been developed for optimizing the topology of a contact-aided compliant mechanism [8]. However, we are not aware of works considering a general methodology for the optimization of grippers and flexible manipulators leveraging self-contacts.

Contribution:

This paper introduces two main contributions: the demonstration of an optimization framework for soft robot design with both self-contacts and external contacts, as well as the analysis of the potential of using self-contacts for soft robot design. The aim is not to design an advanced gripper but to work with a design space parameterization that enables highlighting the contribution of self-contacts to the gripper's performances. This practical design is easily manufactured. Both the simulation and numerical optimization results are experimentally validated.

Additionally, an environment targeted toward soft gripper optimization for grasping tasks is introduced. Although a case study based on a particular parameterization is analyzed in this work, both simulation and grasping quality metrics generalize to other soft grippers. All the code is available as part of the open source plugin *SoftRobots.DesignOptimization* [9] for SOFA, initially intro-

*Univ. Lille, Inria, CNRS, Centrale Lille, UMR 9189 CRIStAL, F-59000 Lille, France. †Instituto de Ciencias de la Ingeniería of the Universidad de O'Higgins, Rancagua, Chile. Tanguy Navez would like to acknowledge the support of both the Region Hauts de France and the ANR through the program AI_PhD@Lille co-funded by the University of Lille and Centre Inria de l'Université de Lille. This research work was partially financed by the EquipEx+ TIRREX project, grant ANR-21-ESRE-0015.

duced in [10]. It also shows how heuristic-based algorithms implemented in the toolbox can be applied to the calibration of mechanical parameters of soft robots in the practical case of the soft grippers. It is especially relevant in cases with non-smooth events such as contact, in which gradient-based methods might struggle with highly non-convex fitness function landscapes. Finally, the flexibility of the proposed framework is highlighted in the design optimization of soft finger shapes for handling different objects.

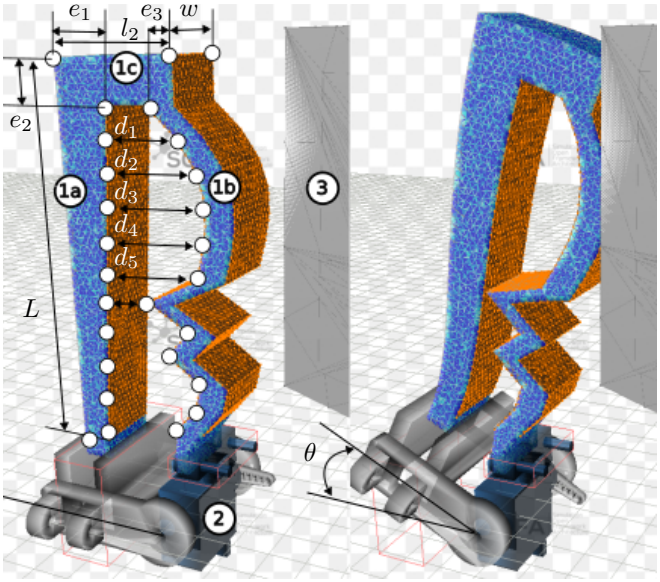

Fig. 1. Illustration of the finger design parameterization. Finger composed of left (1a), top (1c), and right (1b) walls. (2) Servomotor. (3) Example of object to grasp, fixed in space. Left: rest configuration. Right: closed configuration.

II. Methodology

A. Parametric design

The design topology is chosen to enable the creation of self-contacts for specific actuation values during optimization, while being simple enough to understand their effect on the finger performances, and simple to fabricate and actuate. The finger design is depicted in Fig. 1. It consists of two legs attached to a top wall, one being fixed in space at its base and intended to come into contact with the object to grasp, and the other being actuated using a servo motor. The design parameters to optimize are the thickness of each leg and the top wall (e_1, e_2, e_3) and the distances $(d_1, ..., d_n)$ between the left leg and n intermediate points along the right leg. Varying these distance values enables the production of zigzag patterns on the right leg to create self-contacts and adapt to the shape of the object to grasp. Additionally, the finger shape is an extruded planar pattern and is therefore easy to fabricate using additive manufacturing techniques. The design parameters are constrained in intervals with fixed boundaries to prevent interpenetration, limit the finger size, and respect the minimum thickness that can be obtained using the 3D printer considered in this work. The total finger thickness w, the finger width l_2, and the length L are fixed for simplicity.

B. Quasi-Static Finite Element Modeling and Forward Simulation

The quasi-static behavior of the soft finger is simulated using the SOFA Framework and its SoftRobots plugin [11]. The mechanical behavior of the soft gripper deformation is described using continuum mechanics for which there are no analytical solutions in the general case, justifying the use of non-linear FEM for obtaining an approximate solution. Under the assumptions of both low robot acceleration and velocity, using the quasi-static equilibrium is enough for accurately modeling soft robot behavior. It is written as follows:

$$\begin{bmatrix} K_{DD}(x_i) & K_{DR}(x_i)J & 0 & H_c^T \\ J^T K_{RD}(x_i) & J^T K_{RR}(x_i) J & H_a^T & 0 \\ 0 & H_a & 0 & 0 \\ H_c & 0 & 0 & 0 \end{bmatrix} \begin{bmatrix} \Delta x_i \\ \delta_a \\ \lambda_a \\ \lambda_c \end{bmatrix} = \begin{bmatrix} f_{ext} - f_{int}(x_{i-1}) \\ J^T(f_{ext} - f_{int}(x_{i-1})) \\ \theta \\ \delta_c \end{bmatrix} \quad (1)$$

Δx_i are small displacement of nodes around their current position x_i, J is the Jacobian, K_{ij} are the tangent stiffness matrices depending on the current positions of the FEM nodes where D and R refer respectively to deformable and rigidified degrees of freedom. Rigidified nodes are the ones fixed to the servomotor. f_{ext} are gravity forces and f_{int} are nonlinear internal forces of the deformable structure computed from the material constitutive laws. Considering both the low thickness of the finger's leg and the low angle values achieved with the servo-motor, the deformation inside the material is assumed to be small and the material to be elastic linear. Its behavior is characterized by a Poisson ratio ν and a Young's Modulus E. Both actuation and contact constraints effects are integrated into the model as Lagrange multipliers, denoted respectively λ_a and λ_c, whereas the corresponding constraints displacements are δ_a and δ_c. They respectively depict the angular displacement of the servomotor and the distance between contact points computed with the model. The angle θ is the desired servomotor angular displacement specified by the user. Finally, the symbol $\perp$ is used for referring to complementary constraints such as contacts.

The servo motor is modeled using stiffness projection of the node elements of the soft finger parts attached to the actuation device. The degrees of freedom of the rigid part are then directly given by the angular displacement δ_a imposed on the servomotors.

Specific meshes of the soft finger and the manipulated object are provided for modeling collisions. Contact points and surfaces are detected at each time step using a collision detection algorithm. The constraint response is then computed using Signorini's law and friction is modeled using the Coulomb law with a friction coefficient μ.

Solving the constraints is done in two steps by first solving a free configuration of the robot without any constraint:

$$K(x)\Delta x_i^{free} = f_{ext} - f_{int}(x_{i-1}) \quad (2)$$

and then computing the new shape of the robot from δ_a. The motor torque λ_a is then computed.

C. Fitness functions for calibration

Calibration of mechanical parameters is a crucial step for ensuring that the simulation is reliable enough for the targeted applications. Because of the non-linearities and non-smooth events induced by both self-contacts and elastic material behavior, heuristic-based algorithms are suitable for exploring the space of mechanical parameters.

For this purpose, the general idea is to build a fitness function as a distance between sensor measurements on the physical prototypes and the same measurements obtained from the simulation. For the considered soft finger, the servomotor torque is measured and used for calibration. This gives the following fitness function:

$$F^{calib\_torque}(p) = \sqrt{\frac{1}{N}\sum_{\theta_i}(\lambda_a(p,\theta_i) - \lambda_a^*(\theta_i))^2} \quad (3)$$

where p is a vector containing the optimized design parameters, θ_i are the sampled angular displacements imposed on the servomotor, N is the total number of measures, λ_a and λ_a^* are respectively the servomotor torques computed through simulation and measured on the physical prototype.

D. Fitness functions for design optimization

Several metrics have previously been used for assessing soft grippers and manipulators, considering whether object shape matching [12], grasping forces [13], workspace [14] or sensing [10]. When designing a soft gripper finger, the best compromise between its abilities to deform to easily reach the target object to manipulate and to apply forces during the grasping has to be found. One objective is also to reduce the necessary electric energy needed for both actions. Finally, actuation limits in terms of maximum force and torque are taken into account to avoid oversizing the actuation system. These compromises are expressed in the form of three fitness functions to be optimized for the design parameters $p = (e_1, e_2, e_3, d_1, ..., d_n)$.

In order to evaluate these fitness functions, a direct simulation where an angular displacement θ^{max} is imposed at the base of the finger is implemented. The angular displacement θ is gradually increased and the resulting torque is monitored at each simulation time step. The angular displacement samples are denoted θ_i. When the maximum torque is reached, the fitness functions are then computed. The expressions of these three functions are introduced below.

The first function to optimize is the maximum contact force applied by the soft finger on the object, denoted F^{str}. Only the component along the x-axis i.e. the direction from the finger towards the object, is considered. In simulation, this objective is computed as being the sum of the forces $\lambda_{c,x}^j$ exerted on each node of the finger mesh colliding with the nodes of the object at equilibrium:

$$F^{str}(p, \theta^{max}) = \sum \lambda_{c,x}^j \quad (4)$$

The second function directly relates to the necessary energy for maintaining the object during the grasp. It is computed as a resistance F^{grasp_res} to be minimized. To encourage the creation of designs with an effective grasp at the smallest actuation cost, the minimum of the computed resistance for each angular displacement is kept. This gives:

$$F^{grasp\_res}(p) = min_{\theta_i}(\frac{\lambda_a(p,\theta_i)}{F^{str}(p,\theta_i)}) \quad (5)$$

Finally, the F^{grasp_ener} is a metric proportional to the electric energy needed for grasping the object. The torque $\lambda_a(p,\theta_i)$ is measured for each angular step θ_i. For a specific angular displacement, the mechanical work is:

$$E(p,\theta_i) = \lambda_a(p,\theta_i)\theta_i \quad (6)$$

This mechanical work is directly proportional to the electric energy absorbed by the actuator by a constant transmission ratio. Under the hypothesis of constant torque in a sampled angular interval, the total electric energy F^{grasp_ener} absorbed during the grasping cycle can be represented by:

$$F^{grasp\_ener} = \sum_{\theta_i} \lambda_a(p,\theta_i)\theta_i \quad (7)$$

E. Optimization algorithm

The design system we defined is a multi-objective problem with highly non-linear fitness functions regarding design parameters and without available analytical gradients. Heuristic-based algorithms such as Evolutionary and Bayesian algorithms are therefore good candidates for exploring a bounded design space. We use the solver implemented in the *Optuna* library [15]. The expected outcomes typically take the shape of a Pareto front enabling selection of the best compromise between the considered metrics. In our experiments and with our choices of algorithms and hyperparameters, the used Bayesian algorithms are usually better at giving good solutions in a few optimization iterations as they privilege exploitation over exploration. Nevertheless, evolutionary algorithms are mainly used for generating the results in this work for their didactic purpose. Indeed, they enable exploring more in-depth what are good and bad results regarding the fitness metrics.

III. Numerical analysis

A. Design Optimization Results and Analysis

The considered scenario consists of grasping a vertical hexagon-shaped rigid object. For the optimization, a Young's Modulus of $3.62\,\mathrm{MPa}$ and a Poisson's Ratio of 0.452 are selected. They are obtained through torque calibration as described in section IV-B. Moreover, strong hardware constraints come from the maximum torque exerted by the chosen servomotors. Preliminary experimental studies have shown it to be a limiting factor in the angular displacement of the finger when interacting with objects. A maximum torque of $\lambda^{max} = 1.2\,\mathrm{N\,m}$ is thus considered. A single friction coefficient is taken equal to 0.85 for all contacts. These hypotheses are further discussed in section III-C. For a given set of design parameters, the three objectives are assessed using a 3D mesh with a constant density, resulting in a number of nodes varying from 2000 to 3000 with the design.

A total of 40 intermediate angular positions θ_i are sampled in the range [0°,30°]. With these settings, evaluating a design takes between 30 s to 90 s with our setup [1], depending on the number of contact surfaces met during the grasping trajectory.

Both algorithm's hyper-parameters and results obtained for the three fitness functions introduced in section II-D are displayed in Fig. 2.

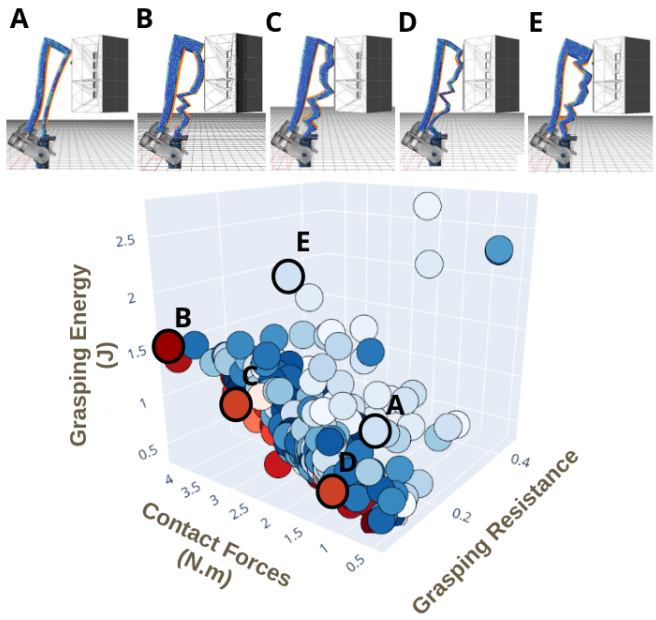

Fig. 2. Pareto Front and a few sampled geometries at the grasping pose obtained for 300 trials of the Soft Finger design optimization. Pareto optimal solutions are represented by red dots. Results are generated using the NSGA-II algorithm with an initial population of 50 design candidates, probabilities of crossover, and swapping parameters between parents of 0.9 and 0.5, respectively.

For generating high contact forces, the best performing results, such as designs **B** and **C**, are the ones with thicker walls and self-contacts, leading to a higher rigidity when contacting the object. The respective designs **D** and **A** are examples of ineffective designs.

The relevance of both the grasping resistance and the grasping energy metrics is now highlighted. On the one hand, poor grasping resistance scores reflect designs where keeping the grasped position is expensive in terms of actuation effort. It is the case for design **A** where the absence of self-contacts does not enable to rigidify the finger enough. It is also the case for design **E** where self-contacts appear too close to the base of the soft finger structure, then directly opposing to the servomotor course. On the other hand, minimizing the grasping energy enables the exclusion of designs where self-contacts appear too soon when the soft finger is closing on an object, as it is the case for **E**. Finally, efficient designs also feature large contact surfaces shared between the soft finger and the considered object. Good compromises between all metrics are designs **B** and **C**.

[1]Laptop with eight cores 2.70 GHz Intel Core i7 - 6820

B. Influence of relative object pose and shape

The potential of self-contacts to adapt to objects with different poses and shapes, as well as the modularity of the design optimization framework, are here demonstrated. Indeed, changing both these parameters has a strong impact on the optimization outcomes.

First, two different object-shape scenarios are considered: one with a horizontal hexagon-shaped object and one with a spherical object. The choice of these object shapes is to explore two different scenarios: one involving contacts with a plane, which is one of the simplest cases, and another one featuring contacts with a small convex surface. This last scenario aims to favor the emergence of designs that wrap around the object to develop more grasping forces. The approach is fairly general and can be extended to any other object shape. In order to favor the appearance of contact surfaces with a specific object shape, a value of 40° for the maximum angle command of the servomotor is considered. Design optimization results are displayed in Fig. 3.

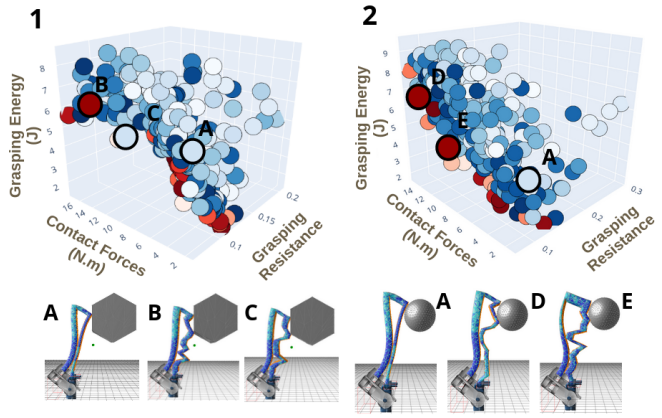

Fig. 3. Pareto Front and a few sampled geometries at the grasping pose obtained for 300 trials of the Soft Finger design optimization for different objects scenarios. Scenarios are 1) a horizontal hexagon-shaped object and 2) a spherical object. Pareto optimal solutions are represented by red dots. Results are generated using the NSGA-II algorithm with an initial population of 50 design candidates, probabilities of crossover, and swapping parameters between parents of respectively 0.9 and 0.5.

Compared with the results in Fig. 2 for the baseline finger design **A**, the considered actuation angle leads to self-contacts during grasping. However, this design still gives poor performances for both object shapes, due to the finger slenderness and the proximity of the contact to the base.

In the hexagon-shaped scenario, because of the object layout, there is little room for generating large contact areas shared between the soft finger and the object unlike in the previous experiment. Only one or two contact lines along the width of the finger are possible at most. This is why the best-performing designs feature double closed kinematic chains for transmitting more contact forces, as shown in both designs **B** and **C**.

For the spherical object, Pareto designs such as designs **D** and **E** both comply with the shape of the object and feature an internal closed chain far away from the base of the finger

and close to the object for an enhanced stiffening. However, **E** is also an example of a design where a second internal closed chain appears too close to the finger base and opposes its course: because of the maximum servomotor torque, only a maximum angular displacement of $35°$ is reached.

C. Influence of friction

The impact of the chosen friction coefficients μ for both soft finger self-contacts and contacts with the object is now discussed. Numerical values of the fitness functions for different designs and friction coefficients are displayed in Table I.

Decreasing the friction coefficient results in reducing the generated contact force and increasing the grasping energy as illustrated in the cases of both designs Fig.2.B and Fig.3.E. This can be explained by the fact that generated forces are lost in sliding motion. However, some designs may take advantage of an increased sliding motion to generate additional contact surfaces. This is particularly the case in manipulation tasks considering small objects such as the sphere. Without necessarily decreasing the contact force, considering altering the μ coefficient and maximizing this contact surface with an additional fitness function would ensure more stable grasping. In practice, these coefficients may be easily altered on the physical prototype by installing pads of different materials located at the expected contact areas on the soft finger. It is interesting to notice that the optimization tools are able to find solutions that go against normal intuition: one would think that increasing friction is always beneficial for stable grasping, as suggested by Table. I, but we show here that this is not always true as it impacts the number of contact surfaces.

IV. Experimental Study

A. Experimental setup

The experimental test bench used to characterize the finger design is represented in Fig. 4 This setup incorporates a Herkulex DRS-0101 servomotor (DFRobot) with a stall torque of $1.18\,\mathrm{N\,m}$ and a resolution of $0.321°$ to actuate the finger. The actuation torque is evaluated using a strain gauge placed on the servo motor arm and by multiplying the measured torque by the arm length. The gauge is capable of measuring forces up to 1 kg with a measurement accuracy of $\pm 0.02\%$, connected to a high-precision 24-bit hx711 analog-to-digital converter. As a result, torques up to $0.36\,\mathrm{N\,m}$ can be measured with an accuracy of $\pm 7.2 \times 10^{-3}\,\mathrm{N\,m}$. The servo motor control and torque estimation are performed on an Arduino Mega acquisition board connected to a PC. This test bench incorporates also a Velleman precision balance enabling precise readings of the contact force with a precision of $9.81\,\mathrm{mN}$; The rest of the components making up the test bench were produced on a Prusa MK3 3D printer using PLA as the material. All the fingers tested were 3D printed (Prusa mk3) using FilaFlex flexible filament with a shore hardness of 60A and a stretch capacity of around 950%.

As the ultimate aim of the test bench was to check the gripping capacities of the various finger designs, a complete gripper was developed, shown in Fig. 5. This gripper uses the same servomotor-finger assembly concept as in Fig. 4, which is repeated 2 times with a $120°$ offset. Its modular design makes it easy to change the design of the fingers using the various fixing and locking screws and to adjust their distance from the gripper center. Different distance values are indicated using 3D-printed graduations for accurate positioning. In order to carry out grasping operations, this gripper was assembled on the end-effector of a UR3 robot arm (Universal Robot). The integration of the gripper enables various 'pick and place' processes to be carried out with objects of different sizes, shapes, and weights.

Design	μ	F^{str}	F^{grasp_res}	F^{grasp_ener}
B from Fig.2	0.85	4.32	0.075	1.49
B from Fig.2	0.30	3.09	0.086	1.40
E from Fig.3	0.85	11.08	0.090	4.32
E from Fig.3	0.30	8.97	0.094	7.14

TABLE I

Fitness functions values for a two soft finger design and different friction coefficient ν.

B. Simulation calibration

The previously mentioned optimization toolbox can also be used to calibrate the model parameters of a soft robotic system involving contacts. In this work, the mechanical properties of the material composing the finger, i.e. E and ν, as well as the distance from the finger d_o to the object and the torque offset τ_0 must be estimated. The Young's modulus is computed from the shore hardness given by the filament manufacturer using the relation in [16], giving, $E = 3.62\,\mathrm{MPa}$. The Poisson ratio and the two other parameters are obtained through optimization, using the fitness function (3). The Poisson ratio is typically close to 0.5 for rubber material, and small changes around these values can lead to large changes in the simulated robot behavior. Therefore, the algorithm is forced to explore values close to

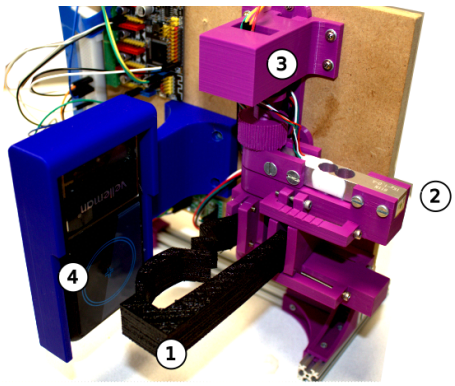

Fig. 4. Experimental setup for the finger design (1). Test bench consisting of a strain gauge (2), a Herkulex drs-0101 servomotor (3) and a Velleman precision balance (4).

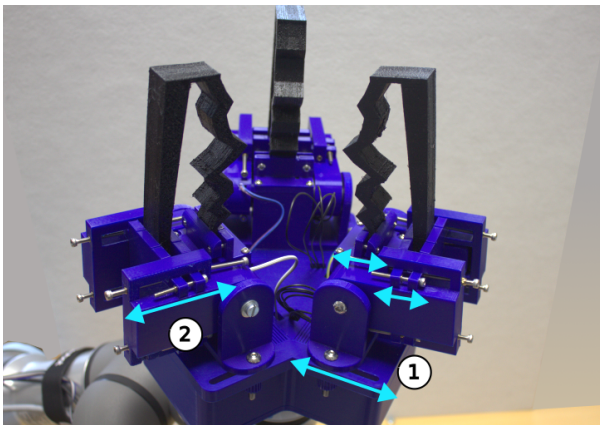

Fig. 5. Prototype of gripper composed of three fingers. Screws and graduation are used to adjust the distance between the finger and the gripper center (1) and the finger width (2). The gripper is assembled on the UR3 collaborative robot in a pick-and-place situation.

0.5 by optimizing a modified Poisson ratio ν_o in the range $[0, 1]$ such as:

$$\begin{aligned} \nu &= (\nu_\infty - \nu_m)(1 - e^{-\frac{\nu_o}{\tau}}) + \nu_m \\ \tau &= -1/\ln\left(1 - \frac{\nu_M - \nu_m}{\nu_\infty - \nu_m}\right) \end{aligned} \tag{8}$$

where $[\nu_m, \nu_M, \nu_\infty] = [0.4, 0.499, 0.501]$ are the values of ν for $\nu_o = [0, 1, \infty]$.

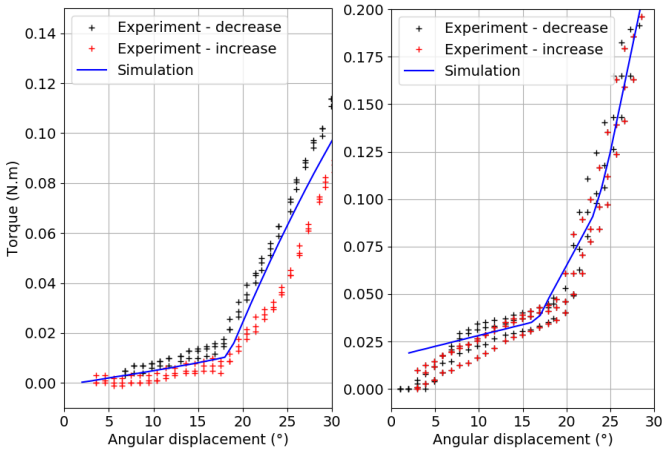

Fig. 6. Measured and simulated relations between angular displacement and torque for the base finger (left) and the C finger (right).

Experimental data was acquired on both the baseline and finger design C from Fig.2. On the test bench, the servomotor's angle was increased and then decreased in the range $[0°, 40°]$ with steps of $1°$. Each experiment was repeated 3 times, leading to point clouds with hysteresis patterns as shown in Fig 6. The centerline of these two point clouds, one for each finger, was extracted using a recursive barycentric method and evaluated at 8 angular displacement values in $[0°, 30°]$, giving the experimental torque values $\lambda_a^\star$. To reach the function minimum as fast as possible, the Tree-Structured Parzen Estimator Bayesian algorithm was used. After 250 iterations, the cost function reaches an acceptable value of $4.3 \times 10^{-3}\,\mathrm{N\,m}$ with the parameters $(\nu, d_o, \tau_0) = (0.451, 35.3\,\mathrm{mm}, -3.2 \times 10^{-3}\,\mathrm{N\,m})$ for the base finger design, and $(0.451, 30.3\,\mathrm{mm}, 1.5 \times 10^{-2}\,\mathrm{N\,m})$ for the C finger design. The obtained value of the Poisson ratio is consistent with the usual values for elastomer materials. The relatively high torque offset observed during the C finger calibration is due to the amplifier of the hx711, whose offset was observed to increase with its temperature. Moreover, the distance to the object varies reasonably around the nominal value of $30\,\mathrm{mm}$, considering the possible assembly and manufacturing defaults on the test bench and the 3D printing errors on the finger. This validates the ability of the model to predict the finger's behavior both when colliding with the object and when self-contact occurs.

C. Performance validation

To validate the performances of the finger designs, the fitness functions values obtained experimentally and numerically are compared. For the comparison, the numerical values of the performance indicators are obtained in simulation with the calibrated parameters determined in section IV-B for the baseline design. The results are presented in Table II. There is a good agreement between the simulated values of grasping energy and the reality, as they depend on the calculated torques that were calibrated. There is a significant difference in contact force for the two designs with self-contacts, leading to discrepancies in the values of grasping resistance as well. After investigation, several sources of error were detected. There are variations of the effective finger length and the relative finger-to-object distance due to manual assembly, leading self-contacts to happen for higher angular displacements and decreasing the final contact force. Also, simulation parameters such as the friction coefficient μ and the density of the surface contact meshes were not optimized. A lower value of μ and a denser mesh significantly reduce the simulated contact force, decreasing further the gap of measured contact forces between simulation and reality. Furthermore, the assumption that both internal and object contacts share the same friction coefficient creates errors as well. However, despite this difference in contact force, finger designs A, C, and B in this order have increasing contact forces and decreasing grasping energy as expected from the Pareto front in Fig. 2. In conclusion, the experiments confirm that the optimization process yields correct sim-to-real behavior in terms of the relative performance of the designs.

D. Grasping demonstration

Designs are demonstrated on a pick-and-place task corresponding to grasping a weighted cylinder and moving it to a given location. In order to have friction coefficients consistent with those used in simulation, tabs of the same material as the fingers are glued to the cylinder in the places where it is gripped. The final angle command imposed to all servomotors is $37°$. The video of the grasping experiments

Design	F^{str}		F^{grasp_res}		F^{grasp_ener}	
	Sim.	Exp.	Sim.	Exp.	Sim.	Exp.
A	0.65	0.63	0.154	0.155	0.296	0.308
B	4.32	0.87	0.075	0.320	1.49	1.247
C	1.88	0.69	0.142	0.430	0.654	0.769

TABLE II

FITNESS FUNCTIONS VALUES FOR THE THREE SOFT FINGER DESIGNS OBTAINED EXPERIMENTALLY (EXP.) AND IN SIMULATION (SIM.).

is available here [17]. The gripper is tested with the designs **A**, **B** and **C** from Fig.2, and manages to lift respectively 150g, 650g, and 750g. The fact that the gripper performs better with design **C** rather than design **B** is explained by the considered greater angle control than the one considered during the optimization. The results obtained validate the superior performances of the optimized designs with self-contacts. Pictures of the gripper design **C** taken at different times during the grasping scenario are provided in Fig. 7.

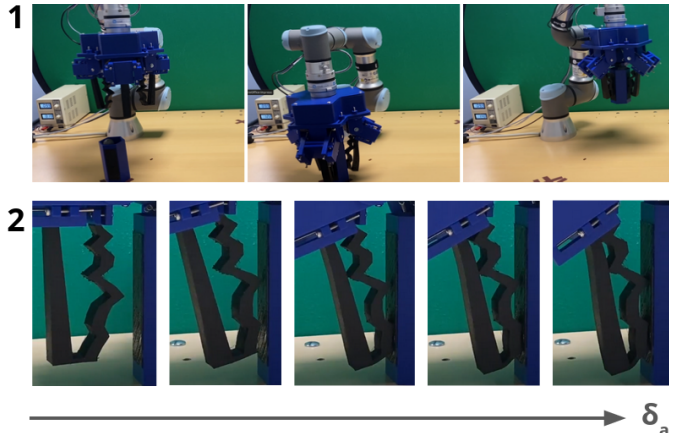

Fig. 7. 1) Gripper design **C** at different moments of the considered grasping scenario, respectively at the initial position, once the object is grasped, and during object displacement. 2) Gripper design **C** during the grasping phase for different angular displacements.

V. CONCLUSIONS

In this article, the computational design of a parametric soft finger, leveraging contact conditions, is explored. Design optimization considering contact conditions is challenging, because of the non-convex nature of the optimization problem when contacts are involved. The optimization task is solved with the help of a previously proposed toolbox, that uses a FEM-based simulation to evaluate the cost functions. We show that the best-performing designs make effective use of self-contacts, both for improving grasping metrics and for adapting to the object shape. The designs were validated experimentally, confirming the plausibility of the Pareto front resulting from simulation with real fabricated design. Thus, more generally, we show that is feasible to address design optimization challenges in Soft Robotics involving contacts with the proposed tools.

Several perspectives are considered to continue this line of work. The considered design parameterization leads to sharp line-shaped contact areas. This strengthens the influence of friction at both the Finger-Finger and Finger-Objects interfaces. In future iterations, we plan to consider building smooth elbow-shaped surfaces between the control points instead of lines, by using Bezier curves for instance.

Also, the design optimization of a soft finger shape is done for a single specific object shape. In future work, we plan to extend the introduced tools for designing a more universal soft gripper, by considering the evaluation of fitness functions averaged on a dataset of different objects. Moreover, other fitness functions may be considered for accounting whether for manufacturing constraints such as minimizing the material volume needed for building the finger, or functional constraints such as the grasping stability i.e. maximizing the shared surface area between the soft finger and object.

REFERENCES

[1] Hughes, Josie, et al. "Soft Manipulators and Grippers: A Review." Frontiers in Robotics and AI, vol. 3, 2016, https://www.frontiersin.org/articles/10.3389/frobt.2016.00069.

[2] Teeple, Clark B., et al. "Multi-Segment Soft Robotic Fingers Enable Robust Precision Grasping." The International Journal of Robotics Research, vol. 39, no. 14, 2020, pp. 1647–67

[3] Manti, M., et al. "Stiffening in Soft Robotics: A Review of the State of the Art". IEEE Robotics & Automation Magazine, vol. 23, no. 3, September 2016, pp. 93106

[4] Mosadegh, Bobak, et al. (2014). Pneumatic networks for soft robotics that actuate rapidly. Advanced functional materials, 24(15), 2163-2170.

[5] Morales Bieze, Thor, et al. "Design, Implementation, and Control of a Deformable Manipulator Robot Based on a Compliant Spine." The International Journal of Robotics Research, vol. 39, no. 14, 2020, pp. 1604–19

[6] Gao, Anzhu, et al. (2020). Modeling and task-oriented optimization of contact-aided continuum robots. IEEE/ASME Transactions on Mechatronics, 25(3), 1444-1455.

[7] Ros-Freixedes, Laura, et al. "Design Optimization of a Contact-Aided Continuum Robot for Endobronchial Interventions Based on Anatomical Constraints." International Journal of Computer Assisted Radiology and Surgery, vol. 14, no. 7, July 2019, pp. 1137–46, https://doi.org/10.1007/s11548-019-01972-8.

[8] Kumar, Prabhat, et al. "Computational Synthesis of Large Deformation Compliant Mechanisms Undergoing Self and Mutual Contact." Journal of Mechanical Design, vol. 141, no. 1, Jan. 2019, p. 012302

[9] Github SoftRobots.Design. `https://github.com/SofaDefrost/SoftRobots.DesignOptimization`.

[10] Navarro, Stefan Escaida, et al. "An Open Source Design Optimization Toolbox Evaluated on a Soft Finger." IEEE Robotics and Automation Letters, vol. 8, no. 9, 2023, pp. 6044–51

[11] Coevoet, E., et al. "Software Toolkit for Modeling, Simulation, and Control of Soft Robots." Advanced Robotics, vol. 31, no. 22, Nov. 2017, pp. 1208–24

[12] Deng, Zhifeng, and Miao Li. "Learning Optimal Fin-Ray Finger Design for Soft Grasping." Frontiers in Robotics and AI, vol. 7, Feb. 2021, p. 590076

[13] Dong, Huixu, et al. "Geometric Design Optimization of an Under-Actuated Tendon-Driven Robotic Gripper." Robotics and Computer-Integrated Manufacturing, vol. 50, Apr. 2018, pp. 80–89

[14] Amehri, Walid, et al. "Workspace Boundary Estimation for Soft Manipulators Using a Continuation Approach." IEEE Robotics and Automation Letters, vol. 6, no. 4, Oct. 2021, pp. 7169–76

[15] Akiba, Takuya, et al. Optuna: A Next-Generation Hyperparameter Optimization Framework. arXiv:1907.10902, arXiv, 25 July 2019

[16] Gent, A.N. "On the Relation between Indentation Hardness and Young's Modulus". Rubber Chemistry and Technology, vol. 31, no. 4, September 1958, pp. 896–906

[17] Attachment video. `https://www.youtube.com/watch?v=7AY0lZ4LyRk`.